



## Original Article

## Asian Pacific Journal of Tropical Biomedicine



apjtb.org

doi: 10.4103/2221–1691.369611

Impact Factor® 1.51

## Salidroside attenuates oxygen and glucose deprivation–induced neuronal injury by inhibiting ferroptosis

Ying–Zhi Li<sup>1</sup>, Ai–Ping Wu<sup>1</sup>, Dan–Dan Wang<sup>1</sup>, Pan–Pan Yang<sup>1</sup>, Bin Sheng<sup>2</sup>✉<sup>1</sup>Department of Rehabilitation Medicine, Zhejiang Hospital, Hangzhou 310007, Zhejiang, China<sup>2</sup>Department of Emergency Medicine, Zhejiang Provincial People's Hospital, Hangzhou 310014, Zhejiang, China

## ABSTRACT

**Objective:** To evaluate the effect of salidroside on oxygen and glucose deprivation (OGD)-treated NT2 cells and its underlying mechanisms of action.

**Methods:** Retinoic acid was used to induce the differentiation of NT2 cells into neurons. The effects of salidroside on survival, apoptosis, inflammatory response, and oxidative stress of neurons undergoing OGD were evaluated. Using precursor cells as controls, the effect of salidroside on the differentiation progression of OGD-treated cells was evaluated. In addition, the effect of erastin, a ferroptosis inducer, on NT2 cells was examined to investigate the underlying mechanisms of neuroprotective action of salidroside.

**Results:** Salidroside alleviated the effects of OGD on neuronal survival, apoptosis, inflammation, and oxidative stress, and promoted NT2 cell differentiation. Moreover, salidroside prevented ferroptosis of OGD-treated cells, which was abolished following erastin treatment, indicating that ferroptosis mediated the regulatory pathway of salidroside.

**Conclusions:** Salidroside attenuates OGD-induced neuronal injury by inhibiting ferroptosis and promotes neuronal differentiation.

**KEYWORDS:** Salidroside; *Rhodiola rosea*; Ferroptosis; Oxygen and glucose deprivation; Neuronal differentiation; Ischemic stroke

## 1. Introduction

One of the most incapacitating and lethal illnesses in the world is

stroke[1,2]. The disease is abrupt and progressive, and it can quickly result in death if the patient is not treated timely. Additionally, survivors tend to experience severe disabilities and ongoing neurological abnormalities[3]. Stroke is divided into hemorrhagic stroke and ischemic stroke[4], with ischemic stroke being the most prevalent[5]. The causes of cerebral ischemia are more complicated, and the frequent causes are stenosis or blockage of the cerebral arteries[6], arterial embolism[7], and hemodynamics[8]. Clinically, intravenous thrombolysis is safe to apply in the treatment of individuals with

## Significance

Salidroside is a phenylpropanoid glycoside derived from *Rhodiola rosea*, which has been found to scavenge free radicals. Mechanisms of neuronal injury in ischemic stroke include inflammation and oxidative stress, which can contribute to long-term neurological dysfunction. The present study shows that salidroside reduces oxygen and glucose deprivation-induced NT2 cell damage by suppressing ferroptosis and promotes NT2 differentiation. Therefore, it can be further explored as a neuroprotective agent in the treatment of ischemic stroke.

✉To whom correspondence may be addressed. E-mail: Shengbin0203@163.com

This is an open access journal, and articles are distributed under the terms of the Creative Commons Attribution-Non Commercial-ShareAlike 4.0 License, which allows others to remix, tweak, and build upon the work non-commercially, as long as appropriate credit is given and the new creations are licensed under the identical terms.

**For reprints contact:** reprints@medknow.com

©2023 Asian Pacific Journal of Tropical Biomedicine Produced by Wolters Kluwer-Medknow.

**How to cite this article:** Li YZ, Wu AP, Wang DD, Yang PP, Sheng B. Salidroside attenuates oxygen and glucose deprivation-induced neuronal injury by inhibiting ferroptosis. Asian Pac J Trop Biomed 2023; 13(2): 70-79.

**Article history:** Received 8 December 2022; Revision 6 January 2023; Accepted 30 January 2023; Available online 24 February 2023

acute ischemic stroke in the absence of contraindications[9]. Nevertheless, the limitations of thrombolytic therapy are demonstrated by the fact that only a small number of patients benefit from it[10–12].

*Rhodiola rosea*, a classic adaptogen, antidepressant, and anti-inflammatory agent, is a medicinal herb originating in Asia and Europe[13–15]. The phenylpropanoid glycoside salidroside, which is derived from *Rhodiola rosea* and utilized in traditional Tibetan medicine, has a wide spectrum of pharmacological effects[16]. Previous research has demonstrated that salidroside can lessen the hypoxia/reoxygenation-induced damage to human cerebral vascular smooth muscle cells[17], as well as the hypobaric hypoxia-induced injury to brain oxidative stress and blood-brain barrier in mice[18]. A disruption in cerebral blood flow in ischemic stroke patients can deprive neurons of oxygen and glucose, leading to neuronal cell loss and neuronal tissue damage[19,20]. The neuronal cell loss or tissue injury following a stroke is permanent and results in long-term neurological impairment since the adult brain has a weak capacity for regeneration[21]. For the study of ischemic stroke, the *in vitro* model of oxygen and glucose deprivation (OGD) is therefore instructive.

Retinoic acid (RA) is a lipophilic small-molecule substance converted from vitamin A, which is crucial for embryogenesis[22]. Studies have shown that RA can boost the proliferation of mouse embryonic stem cells[23]. For developing the central nervous system, RA encourages the differentiation of stem cells towards glial precursor cells and oligodendrocyte-GABAergic neurons[24,25]. The preliminary research of our group indicated that salidroside could boost the percentage of NT2 cells that were differentiated into neurons as a result of RA. Thus, this study aimed to investigate the effect of salidroside on OGD-treated NT2 cells and its underlying mechanisms of action.

## 2. Materials and methods

### 2.1. Cell culture and treatment

NTera-2/D1 (NT2 cells) were obtained from the Cell Resource Center, Institute of Basic Medicine, Chinese Academy of Medical Sciences and cultured in complete medium (Dulbecco's Modified Eagle's Medium containing 10% fetal bovine serum and 1% penicillin-streptomycin), and the medium was changed every 3 d. To induce differentiation, 10  $\mu$ M RA was added to the medium, and cells were passaged every 3 d. Since RA is photosensitive, the RA-treated cells were cultured away from light during the whole experiment. OGD model was established to mimic ischemic injury in stroke. Briefly, cells were cultured in Earle's solution (Procell, Wuhan,

China) without glucose in a 95% N<sub>2</sub> and 5% CO<sub>2</sub> environment for 6 h[26]. Cells were pretreated with salidroside (Nanjing Spring & Autumn Biological Engineering) at concentrations of 10, 25, and 50  $\mu$ M for 1 h[27]. Furthermore, to explore the mediation of ferroptosis, cells were pretreated for 24 h with erastin, a ferroptosis inducer (30 mM, GlpBio)[28].

### 2.2. CCK8 assay

The CCK8 assay was used to assess NT2 cell viability. CCK8 reagent (Abmole) was added to wells of cells treated as above. After 2 h, the absorbance at 450 nm ( $A_{450}$ ) of each well was recorded using a microplate reader (Dojindo Molecular, USA).

### 2.3. Determination of lactate dehydrogenase (LDH)

LDH level was evaluated using an LDH cytotoxicity assay kit (C0017, Beyotime, Shanghai, China). After centrifuging the cell culture plate at 400  $\times g$  for 5 min, the supernatant from each well was obtained as samples. The values were computed using a standard curve.

### 2.4. Assessment of oxidative stress

Assessment of oxidative stress was conducted using the malondialdehyde (MDA, S0131), catalase (CAT, S0051), and glutathione peroxidase (GPx, S0058, Beyotime) assay kits. The NT2 cell lysate was centrifuged at 10000  $\times g$  for 10 min before the supernatant was obtained for detection. The values were computed using a standard curve.

### 2.5. Flow cytometry

Cell apoptosis was assessed with the Annexin V-FITC Apoptosis Kit (Elabscience, Wuhan). Cells were washed twice with phosphate-buffered saline (PBS) before being suspended with 1 $\times$  annexin V binding buffer. Annexin V-FITC reagent and PI reagent were replenished to the suspension, followed by a gentle vortex for 20 min in the dark. The detection was performed using flow cytometry (BD Biosciences, USA).

### 2.6. Western blotting analysis

Nanodrop 2000 (Thermo Fisher) was applied to quantify the proteins isolated from NT2 cells. Protein extracts were resolved by gel electrophoresis and immobilized on PVDF membranes (Millipore). 5% nonfat milk was served as a blocking solution, and membranes were subsequently co-incubated at 4  $^{\circ}$ C with primary

antibodies against Bcl-2 (26593-1-AP; 1:2 000; Proteintech), Bax (AF1270; 1:2 000; Beyotime), cleaved caspase 3 (GTX03281; 1:1 000; GeneTex),  $\beta$ -III-Tubulin (ab18207; 1:500; Abcam), glial fibrillary acidic protein (GFAP) (ab68428; 1:10 000; Abcam), OCT4 (ab181557; 1:1 000; Abcam), PAX6 (ab5790; 1:1 000; Abcam), ferritin heavy chain 1 (FTH1) (ab75972; 1:1 000; Abcam), glutathione peroxidase 4 (GPX4) (ab125066; 1:2 000; Abcam), transferrin (Tf) (AB277635; 1:1 000; Abcam), and  $\beta$ -actin (ab8227; 1:2 000; Abcam) overnight, followed by HRP-linked goat secondary antibody (AB6721; 1:20 000; Abcam) for 2 h. Signal was amplified with enhanced chemifluorescence substrate (GE Healthcare) and the values were analyzed using ImageJ software (National Institutes of Health).

### 2.7. ELISA assay

The levels of tumor necrosis factor (TNF)- $\alpha$  (H052-1), interleukin (IL)-1 $\beta$  (H002), and IL-6 (H007-1, JianCheng, Nanjing) were measured with the corresponding ELISA kits. The supernatant was centrifuged at 500  $\times g$  at 4  $^{\circ}C$  for 5 min and served as samples. A<sub>450</sub> was recorded using a microplate reader.

### 2.8. Immunofluorescence

On the seventh day of RA induction, NT2 cells were fixed with 4% paraformaldehyde and permeabilized with 0.1% Triton X-100 for 30 min. Thereafter, cells were incubated with MAP 2 primary antibody (Abcam) overnight at 4  $^{\circ}C$ , FITC-conjugated goat anti-rabbit antibody for 1 h, and counterstained with DAPI for 5 min. Immunostaining was observed under a fluorescence microscope (Leica, Germany) at 200 $\times$  magnification.

### 2.9. Lipid peroxidation

C11-BODIPY 581/591 is a lipid-soluble fluorescent probe used to indicate lipid peroxidation. C11-BODIPY 581/591 was added to the wells and incubated with cells for 30 min. After being washed twice with PBS, cells were observed under a fluorescence microscope at 200 $\times$  magnification.

### 2.10. Measurement of Fe<sup>2+</sup> levels

The Fe<sup>2+</sup> content in the cells was determined using a ferrous iron Colorimetric Assay Kit (Elabscience). The NT2 cell lysate was centrifuged at 10 000  $\times g$  for 10 min and the supernatant was taken for detection. The values were computed using a standard curve.

### 2.11. Statistical analysis

Data were presented as mean  $\pm$  standard deviation using Prism

8.0 software. Shapiro-Wilk test verified that the data were normally distributed and differences were analyzed by one-way ANOVA followed by Tukey's test.  $P < 0.05$  was considered significantly different.

## 3. Results

### 3.1. Effect of salidroside on cell viability and apoptosis

The effects of different concentrations of salidroside on the viability of OGD-treated NT2 cells were determined using the CCK8 assay. Salidroside at concentrations of 10-50  $\mu M$  did not affect the survival of differentiated NT2 cells (Figure 1A) and increased cell survival after OGD treatment in a concentration-dependent manner (Figure 1B) ( $P < 0.05$ ). In addition, OGD treatment significantly enhanced LDH levels in NT2 cells, whereas salidroside could lower OGD-induced LDH levels ( $P < 0.05$ ) (Figure 1C). Apoptotic levels of NT2 cells were determined by flow cytometry and Western blotting. As shown in Figure 1D-E, OGD treatment significantly increased the percentage of apoptotic cells, accompanied by an increase in Bax and cleaved caspase 3 expression and a decrease in Bcl-2 expression ( $P < 0.05$ ). All these OGD-induced changes were reversed by salidroside in a concentration-dependent manner ( $P < 0.05$ ).

### 3.2. Effect of salidroside on inflammation and oxidative stress

The level of inflammatory factors in the cell supernatant was determined by ELISA. TNF- $\alpha$ , IL-1 $\beta$ , and IL-6 levels were significantly increased in the OGD-treated cells and their levels were decreased by salidroside treatment ( $P < 0.05$ ) (Figure 2A). Meanwhile, OGD treatment increased MDA levels and decreased CAT and GPx levels in NT2 cells. Salidroside treatment abrogated OGD-induced alternations in the levels of these parameters ( $P < 0.05$ ) (Figure 2B).

### 3.3. Effect of salidroside on neuronal differentiation

MAP 2 is a neuron-specific cytoskeletal protein, and the content of MAP 2 in cells was analyzed by immunostaining. RA-induced differentiated cells had significantly higher levels of MAP 2 than untreated cells. The proportion of MAP 2-positive cells was significantly decreased in the group pretreated with OGD ( $P < 0.05$ ), indicating that OGD inhibited cell differentiation. Notably, salidroside relieved the inhibition of cell differentiation induced by OGD ( $P < 0.05$ ) (Figure 3A-B). In addition, differentiation-related cellular markers were detected by Western blotting analysis. The

protein expressions of  $\beta$ -III-Tubulin, GFAP, OCT4, and PAX6 were significantly increased in differentiated cells ( $P < 0.05$ ). OGD treatment reduced the above protein expressions while salidroside could reverse the effect of OGD ( $P < 0.05$ ) (Figure 3C-D).

### 3.4. Effect of salidroside on ferroptosis

Cellular lipid peroxidation levels were assessed using C11-

BODIPY. There was no significant difference between the RA-induced differentiation group and the control group. OGD treatment significantly increased lipid peroxidation in cells, however, salidroside could reduce lipid peroxidation triggered by OGD ( $P < 0.05$ ) (Figure 4A). The levels of  $Fe^{2+}$  and the expression levels of ferroptosis-related proteins were then measured. OGD treatment increased  $Fe^{2+}$  levels in cells ( $P < 0.05$ ). In contrast, salidroside treatment reduced OGD-induced  $Fe^{2+}$  production ( $P < 0.05$ ) (Figure

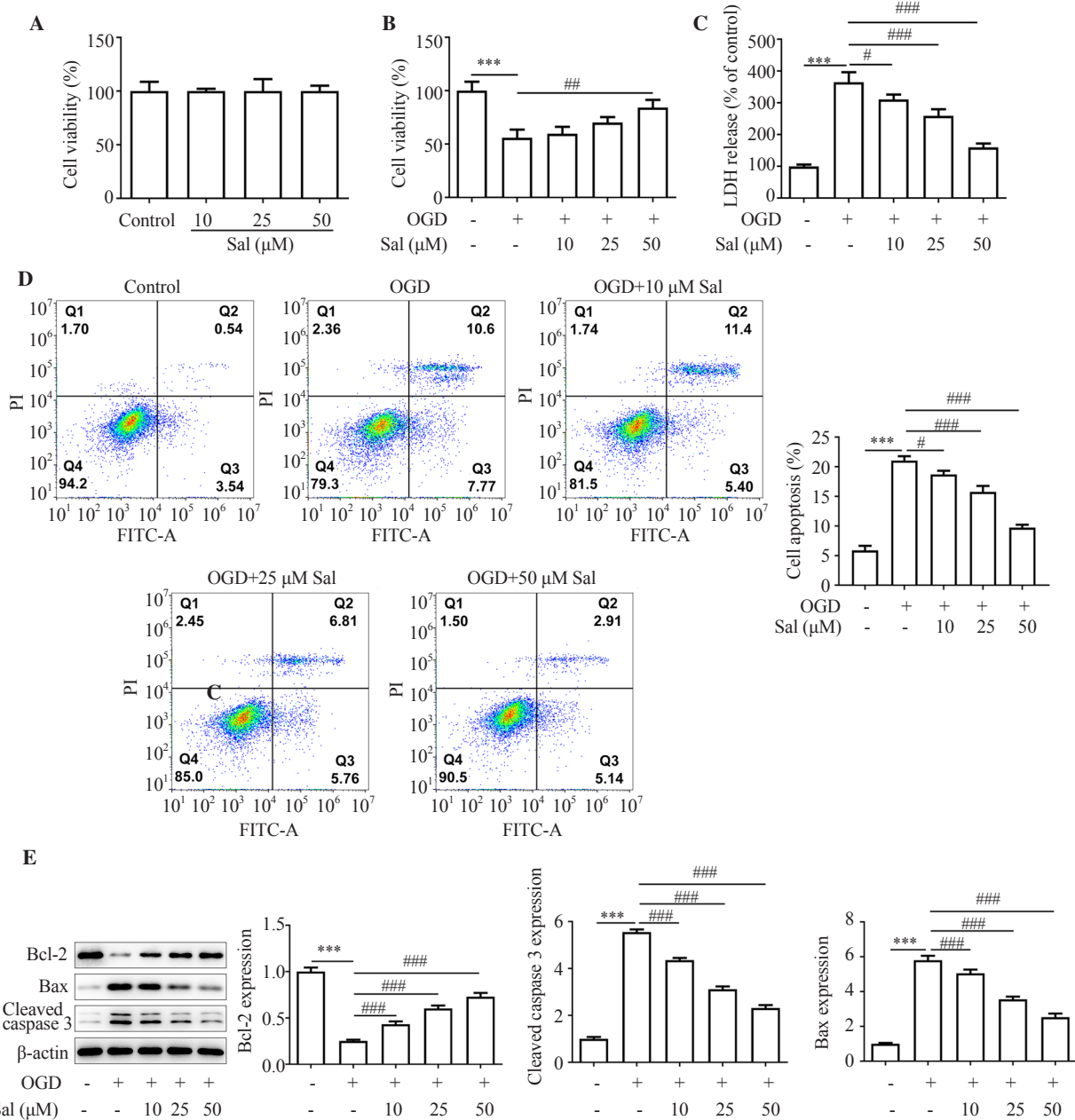


**Figure 1.** Effect of salidroside on the viability and apoptosis in NT2 cells. (A) The effect of different concentrations of salidroside on the viability of normal NT2 cells and (B) OGD-treated NT2 cells was determined using the CCK8 assay. (C) LDH levels in each group of cells were detected by the LDH kit. (D) Apoptosis was determined by flow cytometry. (E) The expression of apoptosis-related proteins was determined by Western blotting analysis.  $\beta$ -actin was used as an internal control. The data are expressed as mean±standard deviation and analyzed by ANOVA. \*\*\* $P < 0.001$  vs. the control group; # $P < 0.05$ , ## $P < 0.01$ , ### $P < 0.001$  vs. the OGD group. Sal: salidroside; OGD: oxygen and glucose deprivation; LDH: lactate dehydrogenase.



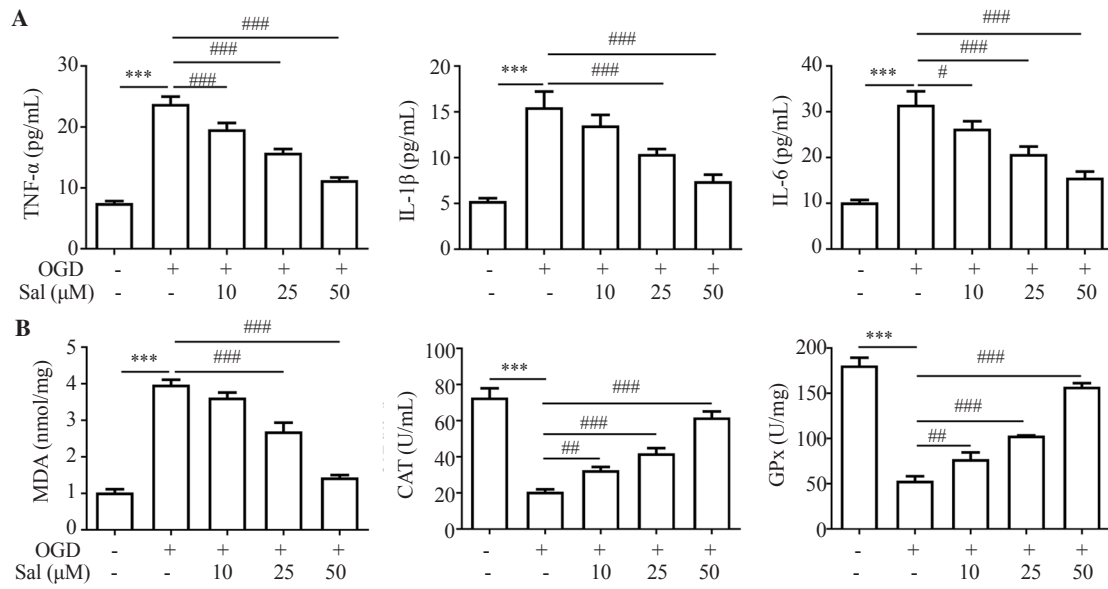


**Figure 2.** Effect of salidroside on inflammation and oxidative stress. (A) The levels of inflammatory factors and (B) oxidative stress markers were determined by ELISA. The data are expressed as mean±standard deviation and analyzed by ANOVA. \*\*\**P*<0.001 vs. the control group; #*P*<0.05, ##*P*<0.01, ###*P*<0.001 vs. the OGD group.

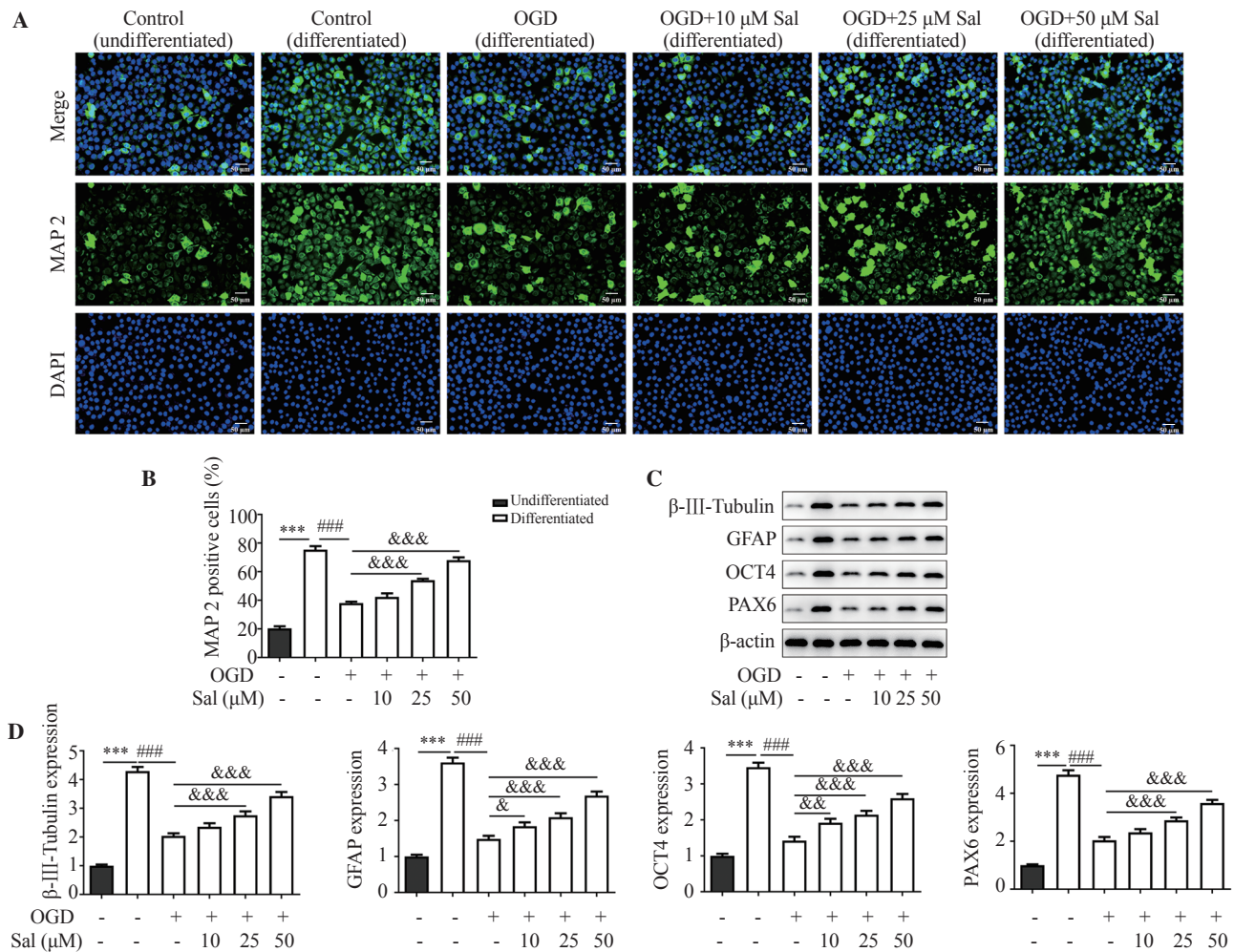


**Figure 3.** Effect of salidroside on neuronal differentiation. (A-B) The proportion of MAP 2-positive cells was analyzed by immunostaining (magnification 200×). (C-D) Differentiation-related cellular markers were detected by Western blotting analysis. β-actin was used as an internal control. The data are expressed as mean±standard deviation and analyzed by ANOVA. \*\*\**P*<0.001 vs. the control group (undifferentiated); ###*P*<0.001 vs. the control group (differentiated); &*P*<0.05, &&*P*<0.01, &&&*P*<0.001 vs. the OGD group. MAP 2: microtubule associated protein 2.

4B). In addition, OGD treatment decreased FTH1 and GPX4 protein expression, and increased Tf expression ( $P<0.05$ ), while salidroside treatment alleviated the alterations in these proteins ( $P<0.05$ ) (Figure 4C).

### 3.5. Mediation of ferroptosis

Cells treated with erastin, a ferroptosis inducer, showed increased LDH levels (Figure 5A), increased number of apoptotic cells (Figure 5B-C), along with increased Bax and cleaved caspase 3 and decreased Bcl-2 compared with the OGD+salidroside group ( $P<0.05$ ) (Figure 5D). Similarly, erastin reversed the effect of salidroside on the levels of inflammatory cytokines and oxidative stress markers ( $P<0.05$ ) (Figure 5E-F). Furthermore, erastin caused a decrease in the proportion of MAP 2-positive cells (Figure 6A-B), and reduced protein expressions of  $\beta$ -III-Tubulin, GFAP, OCT4, and PAX6 ( $P<0.05$ ) (Figure 6C-D).

## 4. Discussion

Despite some treatments, the prognosis for patients with ischemic

stroke remains unsatisfactory. Complex processes have been found to mediate neuronal death, including neuro-inflammation, oxidative stress, excitotoxicity, and apoptosis[29]. Currently, neuronal death and secondary inflammatory responses that occur immediately after ischemia are two key aspects that are being extensively investigated[30,31]. So far, how these two events are coordinated and regulated after ischemia remains to be further investigated. This study suggested that salidroside could improve the survival rate of neurons and reduce the level of inflammatory factors after OGD. This may imply that salidroside can assist neurons in resisting adverse environment-induced death in a rapid time. Cerebral ischemia can lead to damage to the blood-brain barrier and increase the risk of complications secondary to thrombolysis[32-34]. Many studies have shown that intranasal administration is a potential way to directly deliver drugs to the brain[35,36], which can assist more natural medicines developed in herbal medicines to break through the blood-brain barrier in the treatment of brain diseases.

Ferroptosis is a form of programmed cell death characterized by iron-dependent accumulation of lipid peroxides[37]. Biochemical features of ferroptosis include glutathione antioxidant dysfunction, GPX4 depletion, and lipid peroxide accumulation. When lipid peroxides surpass cellular antioxidant activity, they cause protein

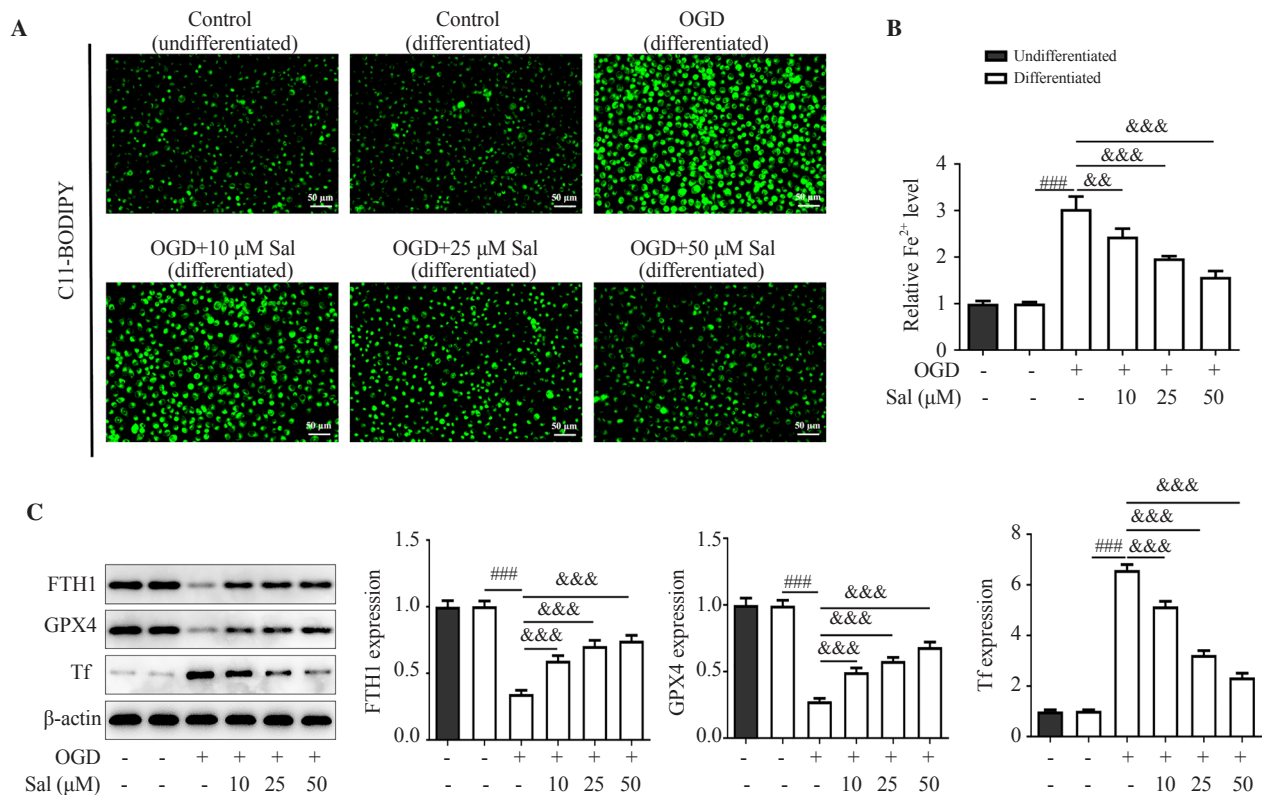


**Figure 4.** Effect of salidroside on ferroptosis. (A) Cellular lipid peroxidation level was assessed using C11-BODIPY (magnification 200 $\times$ ). (B) The level of  $Fe^{2+}$  was measured using an assay kit. (C) The expression levels of ferroptosis-related proteins were measured by Western blotting analysis.  $\beta$ -actin was used as an internal control. The data are expressed as mean $\pm$ standard deviation and analyzed by ANOVA. ### $P<0.001$  vs. the control group (differentiated); &&& $P<0.01$ , &&& $P<0.001$  vs. the OGD group.

collapse, lipid destruction, and neuronal death[38]. Iron chelation therapy has shown efficacy in preclinical ischemic stroke studies[39,40]. Moreover, several *in vivo* and *in vitro* studies have shown that inhibition of ferroptosis is also beneficial in improving hemorrhagic stroke and reperfusion injury[41,42].

The complex development of the mammalian central nervous system relies on various cell types, including neurons, astrocytes, and oligodendrocytes[43]. In the central nervous system, neural precursor cells are pluripotent cells capable of self-renewal and generating neurons, astrocytes, and oligodendrocytes. Neural precursor cells

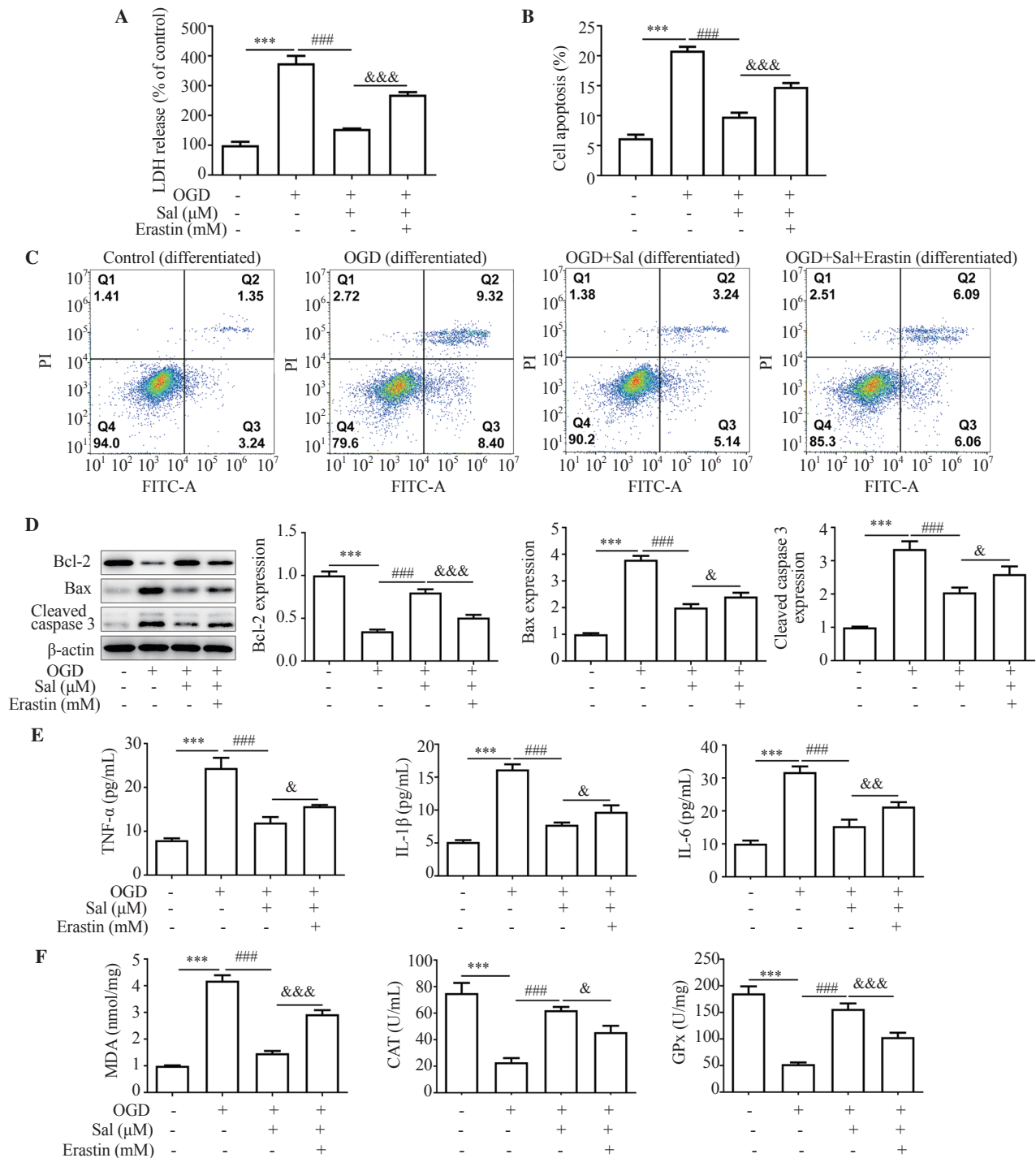


**Figure 5.** Effect of erastin, a ferroptosis inducer, on the viability, apoptosis, inflammation, and oxidative stress in NT2 cells. (A) The LDH levels in each group of cells were detected by an LDH kit. (B-C) Apoptosis was determined by flow cytometry. (D) The expression of apoptosis-related proteins was determined by Western blotting analysis. (E) The levels of inflammatory factors were determined by ELISA kit. (F) The levels of the oxidative stress markers were determined by assay kits. The data are expressed as mean $\pm$ standard deviation and analyzed by ANOVA. \*\*\* $P$ <0.001 vs. the control group; ### $P$ <0.001 vs. the OGD group; & $P$ <0.05, && $P$ <0.01, &&& $P$ <0.001 vs. the OGD+Sal group.

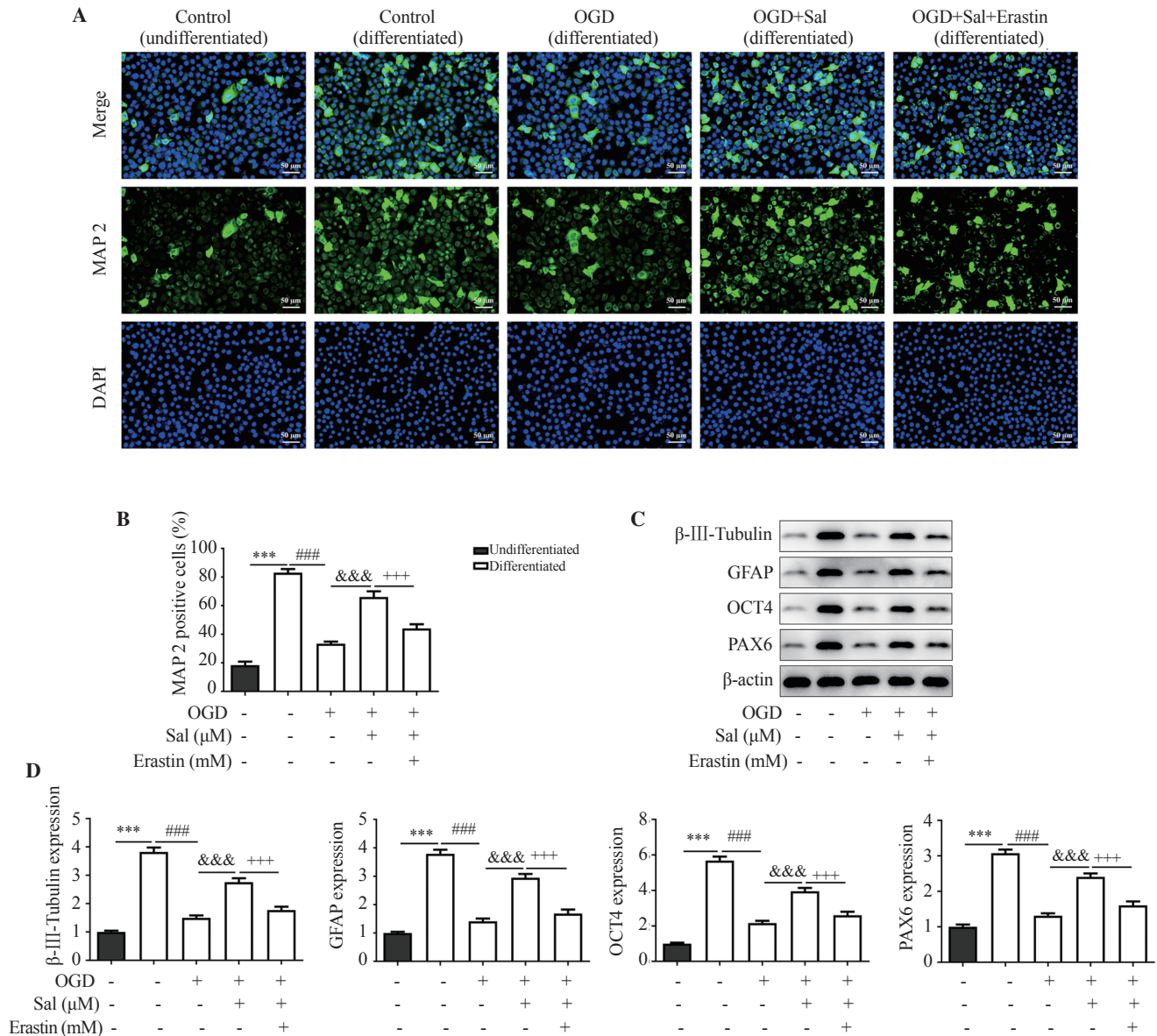


**Figure 6.** Effect of erastin on neuronal differentiation. (A-B) The proportion of MAP 2-positive cells was analyzed by immunostaining (magnification 200×). (C-D) Differentiation-related cellular markers were detected by Western blotting analysis. The data are expressed as mean±standard deviation and analyzed by ANOVA. \*\*\**P*<0.001 vs. the control group (undifferentiated); ###*P*<0.001 vs. the control group (differentiated), &&&*P*<0.001 vs. the OGD group; +++*P*<0.001 vs. the OGD+Sal group.

proliferate, differentiate, migrate, and ultimately form neuronal networks[44]. The NT2 cell line is a human-derived cell with neuronal precursor properties that can be induced to differentiate into neurons[45]. In the present study, salidroside could assist RA to enhance the induction of NT2 differentiation, even after undergoing OGD. The emerging generation of neurons after differentiation can reduce the damage to the nervous system caused by cerebral ischemia, which further illustrates the pharmacological effects of salidroside. Nevertheless, future *in vivo* and clinical experiments should be carried out to further verify its neuroprotective effect.

Taken together, this study reveals that salidroside attenuates OGD-induced damage by inhibiting ferroptosis and promotes

neuronal differentiation. Therefore, it can be further explored as a neuroprotective agent.

### Conflict of interest statement

The authors declare that they have no competing interests.

### Funding

This study was supported by the Zhejiang Traditional Chinese



Medicine Science and Technology Plan Project (2021ZB027, 2023ZL267) and Zhejiang Medical and Health Platform Project of China (2019KY002, 2019RC092).

## Authors' contributions

YZL and APW contributed to the concept, experiments, and draft. DDW, PPY, and BS contributed to the experiments and data analysis. BS contributed to the critical revision of the manuscript. All authors approved the final version.

## References

- [1] Pallesen LP, Barlinn K, Puetz V. Role of decompressive craniectomy in ischemic stroke. *Front Neurol* 2018; **9**: 1119.
- [2] Steigleder T, Kollmar R, Ostgathe C. Palliative care for stroke patients and their families: Barriers for implementation. *Front Neurol* 2019; **10**: 164.
- [3] Barakat W, Fahmy A, Askar M, El-Kannishy S. Effectiveness of arginase inhibitors against experimentally induced stroke. *Naunyn Schmiedebergs Arch Pharmacol* 2018; **391**(6): 603-612.
- [4] Chen ZQ, Mou RT, Feng DX, Wang Z, Chen G. The role of nitric oxide in stroke. *Med Gas Res* 2017; **7**(3): 194-203.
- [5] Campbell BC. Thrombolysis and thrombectomy for acute ischemic stroke: Strengths and synergies. *Semin Thromb Hemost* 2017; **43**(2): 185-190.
- [6] Nakagomi T, Tanaka Y, Nakagomi N, Matsuyama T, Yoshimura S. How long are reperfusion therapies beneficial for patients after stroke onset? Lessons from lethal ischemia following early reperfusion in a mouse model of stroke. *Int J Mol Sci* 2020; **21**(17). doi: 10.3390/ijms21176360.
- [7] Ben RJ, Jao JC, Chang CY, Tzeng JS, Hwang LC, Chen PC. Longitudinal investigation of ischemic stroke using magnetic resonance imaging: Animal model. *J Xray Sci Technol* 2019; **27**(5): 935-947.
- [8] Xiao XT, Luo C, Yuan Y, Xiao L, Qu WS. Systematic evaluation during early-phase ischemia predicts outcomes in middle cerebral artery occlusion mice. *Neuroreport* 2021; **32**(1): 29-37.
- [9] Muir K. No space left for intravenous thrombolysis in acute stroke: CONS. *Intern Emerg Med* 2016; **11**(5): 619-621.
- [10] Nakamura A, Otani K, Shichita T. Lipid mediators and sterile inflammation in ischemic stroke. *Int Immunol* 2020; **32**(11): 719-725.
- [11] Knecht T, Story J, Liu J, Davis W, Borlongan CV, Dela Peña IC. Adjunctive therapy approaches for ischemic stroke: Innovations to expand time window of treatment. *Int J Mol Sci* 2017; **18**(12). doi: 10.3390/ijms18122756.
- [12] Wu C, Wu D, Chen J, Li C, Ji X. Why not intravenous thrombolysis in patients with recurrent stroke within 3 months? *Aging Dis* 2018; **9**(2): 309-316.
- [13] Todorova V, Ivanov K, Delattre C, Nalbantova V, Karcheva-Bahchevanska D, Ivanova S. Plant adaptogens-history and future perspectives. *Nutrients* 2021; **13**(8). doi: 10.3390/nu13082861.
- [14] Pu WL, Zhang MY, Bai RY, Sun LK, Li WH, Yu YL, et al. Anti-inflammatory effects of *Rhodiola rosea* L.: A review. *Biomed Pharmacother* 2020; **121**: 109552.
- [15] Angheliescu IG, Edwards D, Seifritz E, Kasper S. Stress management and the role of *Rhodiola rosea*: A review. *Int J Psychiatry Clin Pract* 2018; **22**(4): 242-252.
- [16] He S, Fan H, Sun B, Yang M, Liu H, Yang J, et al. Tibetan medicine salidroside improves host anti-mycobacterial response by boosting inflammatory cytokine production in zebrafish. *Front Pharmacol* 2022; **13**: 936295.
- [17] Xu L, Jia L, Wang Q, Hou J, Li S, Teng J. Salidroside attenuates hypoxia/reoxygenation-induced human brain vascular smooth muscle cell injury by activating the SIRT1/FOXO3a pathway. *Exp Ther Med* 2018; **15**(1): 822-830.
- [18] Jiang S, Fan F, Yang L, Chen K, Sun Z, Zhang Y, et al. Salidroside attenuates high altitude hypobaric hypoxia-induced brain injury in mice via inhibiting NF-κB/NLRP3 pathway. *Eur J Pharmacol* 2022; **925**: 175015.
- [19] Sekerdag E, Solaroglu I, Gursoy-Ozdemir Y. Cell death mechanisms in stroke and novel molecular and cellular treatment options. *Curr Neuropharmacol* 2018; **16**(9): 1396-1415.
- [20] Brown GC. Neuronal loss after stroke due to microglial phagocytosis of stressed neurons. *Int J Mol Sci* 2021; **22**(24). doi: 10.3390/ijms222413442.
- [21] Kim H, Cooke MJ, Shoichet MS. Creating permissive microenvironments for stem cell transplantation into the central nervous system. *Trends Biotechnol* 2012; **30**(1): 55-63.
- [22] Ghyselinck NB, Duester G. Retinoic acid signaling pathways. *Development* 2019; **146**(13). doi: 10.1242/dev.167502.
- [23] Rochette-Egly C. Retinoic acid signaling and mouse embryonic stem cell differentiation: Cross talk between genomic and non-genomic effects of RA. *Biochim Biophys Acta* 2015; **1851**(1): 66-75.
- [24] Morrison VE, Smith VN, Huang JK. Retinoic acid is required for oligodendrocyte precursor cell production and differentiation in the postnatal mouse corpus callosum. *eNeuro* 2020; **7**(1). doi: 10.1523/ENEURO.0270-19.2019.
- [25] Asano H, Aonuma M, Sanosaka T, Kohyama J, Namihira M, Nakashima K. Astrocyte differentiation of neural precursor cells is enhanced by retinoic acid through a change in epigenetic modification. *Stem Cells* 2009; **27**(11): 2744-2752.
- [26] Song X, Zhang L, Hui X, Sun X, Yang J, Wang J, et al. Selenium-containing protein from selenium-enriched *Spirulina platensis* antagonizes oxygen glucose deprivation-induced neurotoxicity by inhibiting ROS-mediated oxidative damage through regulating MPTP opening. *Pharm*



- Biol* 2021; **59**(1): 629-638.
- [27]Zheng K, Sheng Z, Li Y, Lu H. Salidroside inhibits oxygen glucose deprivation (OGD)/re-oxygenation-induced H9c2 cell necrosis through activating of Akt-Nrf2 signaling. *Biochem Biophys Res Commun* 2014; **451**(1): 79-85.
- [28]Zhang Q, Hu Y, Hu JE, Ding Y, Shen Y, Xu H, et al. Sp1-mediated upregulation of Prdx6 expression prevents podocyte injury in diabetic nephropathy via mitigation of oxidative stress and ferroptosis. *Life Sci* 2021; **278**: 119529.
- [29]Tuo QZ, Zhang ST, Lei P. Mechanisms of neuronal cell death in ischemic stroke and their therapeutic implications. *Med Res Rev* 2022; **42**(1): 259-305.
- [30]Arumugam TV, Baik SH, Balaganapathy P, Sobey CG, Mattson MP, Jo DG. Notch signaling and neuronal death in stroke. *Prog Neurobiol* 2018; **165-167**: 103-116.
- [31]Denorme F, Portier I, Rustad JL, Cody MJ, de Araujo CV, Hoki C, et al. Neutrophil extracellular traps regulate ischemic stroke brain injury. *J Clin Invest* 2022; **132**(10). doi: 10.1172/JCI154225.
- [32]Jiang X, Andjelkovic AV, Zhu L, Yang T, Bennett MVL, Chen J, et al. Blood-brain barrier dysfunction and recovery after ischemic stroke. *Prog Neurobiol* 2018; **163-164**: 144-171.
- [33]Yaghi S, Willey JZ, Cucchiara B, Goldstein JN, Gonzales NR, Khatri P, et al. Treatment and outcome of hemorrhagic transformation after intravenous alteplase in acute ischemic stroke: A scientific statement for healthcare professionals from the American Heart Association/American Stroke Association. *Stroke* 2017; **48**(12): e343-e361.
- [34]Arba F, Rinaldi C, Caimano D, Vit F, Busto G, Fainardi E. Blood-brain barrier disruption and hemorrhagic transformation in acute ischemic stroke: Systematic review and meta-analysis. *Front Neurol* 2020; **11**: 594613.
- [35]Erdő F, Bors LA, Farkas D, Bajza Á, Gizurason S. Evaluation of intranasal delivery route of drug administration for brain targeting. *Brain Res Bull* 2018; **143**: 155-170.
- [36]Battaglia L, Panciani PP, Muntoni E, Capucchio MT, Biasibetti E, De Bonis P, et al. Lipid nanoparticles for intranasal administration: Application to nose-to-brain delivery. *Expert Opin Drug Deliv* 2018; **15**(4): 369-378.
- [37]Hirschhorn T, Stockwell BR. The development of the concept of ferroptosis. *Free Radic Biol Med* 2019; **133**: 130-143.
- [38]Chen X, Kang R, Kroemer G, Tang D. Ferroptosis in infection, inflammation, and immunity. *J Exp Med* 2021; **218**(6). doi: 10.1084/jem.20210518.
- [39]Duan R, Sun K, Fang F, Wang N, He R, Gao Y, et al. An ischemia-homing bioengineered nano-scavenger for specifically alleviating multiple pathogenesis in ischemic stroke. *J Nanobiotechnol* 2022; **20**(1): 397.
- [40]Yu X, Wang Z, Li YV. Metal ion chelation enhances tissue plasminogen activator (tPA)-induced thrombolysis: An *in vitro* and *in vivo* study. *J Thromb Thrombolysis* 2022; **53**(2): 291-301.
- [41]Xu Y, Li K, Zhao Y, Zhou L, Liu Y, Zhao J. Role of ferroptosis in stroke. *Cell Mol Neurobiol* 2023; **43**(1): 205-222.
- [42]Guo H, Zhu L, Tang P, Chen D, Li Y, Li J, et al. Carthamin yellow improves cerebral ischemia-reperfusion injury by attenuating inflammation and ferroptosis in rats. *Int J Mol Med* 2021; **47**(4): 52.
- [43]Xu S, Lu J, Shao A, Zhang JH, Zhang J. Glial cells: Role of the immune response in ischemic stroke. *Front Immunol* 2020; **11**: 294.
- [44]Lim DA, Alvarez-Buylla A. The adult ventricular-subventricular zone (V-SVZ) and olfactory bulb (OB) neurogenesis. *Cold Spring Harb Perspect Biol* 2016; **8**(5). doi: 10.1101/cshperspect.a018820.
- [45]Podrygajlo G, Tegenge MA, Gierse A, Paquet-Durand F, Tan S, Bicker G, et al. Cellular phenotypes of human model neurons (NT2) after differentiation in aggregate culture. *Cell Tissue Res* 2009; **336**(3): 439-452.

## Publisher's note

The Publisher of the *Journal* remains neutral with regard to jurisdictional claims in published maps and institutional affiliations.